Sparkes, R., Tilmann, F., Hovius, N., Hillier, J. (2010): Subducted seafloor relief stops rupture in South American great earthquakes: Implications for rupture behaviour in the 2010 Maule, Chile earthquake. - Earth and Planetary Science Letters, 298, 1-2, 89-94

DOI: 10.1016/j.epsl.2010.07.029

Subducted seafloor relief stops rupture in South American great earthquakes: Implications for rupture behaviour in the 2010 Maule, Chile earthquake.

Robert Sparkes, Frederik Tilmann, Niels Hovius and John Hillier

ABSTRACT

Great subduction earthquakes cause destructive surface deformation and ground shaking over hundreds of kilometres. Their rupture length is limited by the characteristic strength of the subduction plate interface, and by lateral variations in its mechanical properties. It has been proposed that subduction of topographic features such as ridges and seamounts can affect these properties and stop rupture propagation, but the required relief and physical mechanisms of topographic rupture limitation are not well understood. Here we show that the rupture limits of thirteen historic great earthquakes along the South America-Nazca plate margin are strongly correlated with subducted topography with relief >1000m, including the Juan Fernandez Ridge. The northern limit of rupture in the M_w8.8 Maule, Chile earthquake of 27 February 2010 is located where this ridge subducts. Analysis of intermediate-magnitude earthquakes shows that in most places the subduction of high seafloor relief creates weak, aseismic zones at the plate interface, which prevent rupture propagation, but that the Juan Fernandez Ridge is associated with a locally strong plate interface. The maximum rupture length, and thus magnitude, of great subduction earthquakes is therefore determined by the size and lateral spacing of topographic features where they are present on the subducting plate.

Introduction

The amount of displacement in an earthquake is commonly proportional to its rupture length (Wells and Coppersmith, 1994). This determines the area that can be affected by strong ground motion and surface deformation and, where relevant, the amplitude and length scale of associated tsunamis. In most earthquakes, rupture termination is likely to be determined by the energy available for rupture tip propagation along a plane with relatively uniform properties, but for larger potential rupture planes, there is an increased likelihood that mechanical properties vary along the plane. Mechanical heterogeneities could impede rupture tip propagation, or, alternatively, serve as rupture nucleation points. If indeed they exist, these effects may be expected to be most prominent for the largest earthquakes, and they could give rise to segmentation of very long seismogenic fault zones.

Globally, great megathrust earthquakes ($M_w \geq 8.0$) accommodate the majority of shortening along subduction margins. They repeatedly rupture the same margin segments (Beck *et al.,* 1998, Comte *et al.,* 1986), with lengths exceeding the ~100 km width of the seismogenic zone. There are indications that rupture termination in great subduction earthquakes could be forced by along-strike variation of properties of the plate interface (Kelleher and McCann, 1976, Sladen, 2009, Bilek, 2010, in press, Loveless *et al*., 2010, in press). For example, coincidence of some rupture areas of great subduction earthquakes with large negative forearc gravity anomalies along subduction margins has been attributed to localized strong plate interface friction (Song and Simons, 2003, Llenos and McGuire, 2007), and rupture areas have been found to coincide with forearc basins, possibly the surface expression of subduction erosion (Wells *et al.,* 2003, Ranero and von Huene, 2000). However, such forearc features can depend on as well as influence the frictional properties along the plate interface, making it difficult to establish the direction of causality.

Incoming seafloor structures have long been suspected to have an influence on plate interface structure (Cloos, 1992, Scholz and Small, 1997, Bilek *et al.,* 2003). Notably, rupture in the 1946 earthquake along the Nankai trough was deflected around a subducting seamount (Kodaira *et al.,* 2002). This may have been caused by an increase of normal stress, and hence seismic coupling, on the subducted topography (Scholz and Small, 1997), or by the formation of a weak, aseismic area where strain cannot build up (Bilek *et al.*, 2003). Regardless of the mechanism, in the case of subducted seafloor topography the direction of causality is unambiguous. If a correlation between the location of subducted seafloor topography and the extent of earthquake ruptures can be demonstrated then it is clear that the former has influenced the latter by affecting the frictional properties of the plate interface. Although many previous studies have noted the apparent coincidence of incoming seamount chains and earthquake segmentation, the statistical significance of these observations has hitherto not been tested, nor is it clear how large a seamount chain has to be before it can (co-)determine rupture segmentation.

Acknowledging the fact that several other factors may affect rupture propagation along a subduction plate interface, we have sought to isolate and determine the strength and nature of the role of subducted topography in rupture termination in great earthquakes, and the critical size of subducted topography. We have done this by exploring the randomness or otherwise of the collocation of extrapolated seafloor relief, great earthquake rupture limits and patches of subdued background seismicity along the Pacific margin of South America between 12°S and 47°S. On this margin, the Nazca Plate moves eastward at ~65 mm/yr relative to, and is subducted under South America (Angermann *et al.,* 1999). Large sections of the Nazca Plate have smooth seafloor with topographic relief <200 m, but elsewhere seamount chains with varying relief of up to 3.5 km are carried into the subduction trench, enabling a quantitative exploration of the effect of subducting topography on seismicity. Since 1868, 15 great earthquakes have occurred along the Nazca margin (See Fig. 1 and Table 1), including the largest recorded earthquake, M_w9.5 in 1960. These earthquakes had rupture lengths from 150 to 1,050 km. On 27 February 2010, a ~600 km section of the Nazca margin ruptured in the M_w 8.8 Maule earthquake. Here, we demonstrate that the sustained subduction of seafloor features with relief in excess of ~1.0 km has systematically stopped rupture in these historic great earthquakes on the Nazca margin. We argue that in most cases rupture termination is due to the creation of weak, aseismic zones in the plate interface. In addition, we explore the possible causes of rupture termination in the 2010 Maule earthquake. It has not been our intention to carry out a global survey of subduction margins, but although the critical height of subducted topography may vary between settings, its role in stopping earthquake rupture is likely to be similar along the Nazca margin and elsewhere.

Constraints on Rupture Zones and Subducting Topography

Subduction zone earthquakes with M_w<8.0 tend to rupture distances less than 100 km and their rupture zones have aspect ratios close to one. As 100km is comparable to the width of the seismogenic zone, the endpoints of these major but not great earthquakes cannot tell us whether there are features along strike that may have stopped their rupture. Whilst some M_w 7-7.9 earthquakes have ruptured larger distances, in the interest of consistency we have restricted our study to M_w>8.0, as these great events should all have ruptured the plate interface over more than 100 km in the trench-parallel direction, making it possible to identify parts of the plate interface that may have acted as a barrier or nucleation point for earthquake rupture. Earthquakes with M_w<8.0 will be considered in the discussion section.

The anecdotal record of very large earthquakes along the Nazca margin stretches back to at least 1575 (Cisternas *et al*., 2005), but events before 1868 are insufficiently documented to determine the extent of their rupture zones in any detail. Since that year, 15 earthquakes with estimated moment magnitude $M_w \geq 8.0$ have occurred on the margin. For events prior to 1973, rupture zones have been determined from damage intensity and co-seismic subsidence (Kelleher, 1972, Spence *et al.*, 1999, Cisternas *et al.*, 2005), and we have used published estimates (see Table 1), with the exception of the 1908 $M_w 8.0$ earthquake offshore Peru, which is insufficiently documented to be included in this study. After 1973, rupture zones can be constrained from aftershock locations (Wells and Coppersmith, 1994, USGS NEIC catalog). We have done this for all recent great earthquakes, including the 2010 Maule event. Uncertainty in the mapping of rupture zones is due to the gradual decrease of slip toward the rupture tip, and the imperfect correlation between the rupture zone and the distribution of aftershocks, seismic intensities and co-seismic subsidence. The resulting uncertainty is less than 50 km (Kelleher, 1972), and rupture limits determined from aftershock observations match other published rupture area estimates (Comte *et al*., 1986, Delouis *et* al., 1997, Sobesiak, 2000, Tavera *et al.*, 2002) to within 40 km. Our findings are therefore not sensitive to the exact method of defining rupture zones, and this uncertainty cannot be easily reduced for historical earthquakes.

Seafloor topography was constrained from the TOPEX global seafloor bathymetry dataset (Smith and Sandwell, 1997), which is created from satellite altimetry. This dataset was chosen for its consistent derivation of the depth both along the margin and in the open ocean, and for its inclusion of seamounts unmeasured by sonic soundings, but the accuracy of seamount heights may be ±100 m or more (Marks and Smith, 2007). We have calculated seafloor relief by taking the difference between the depth at a point and the mean depth of the seafloor within a radius of 3°, which is generally

~4000 m. The Nazca Plate has prominent topographic features with positive relief >400 m, including the Nazca Ridge (Spence *et al*., 1999), which has relief of up to 3500 m, and several seamount chains with approximately linear trends for >500 km extending to the subduction zone. Assuming some continuity of seamount chain formation through time, it is likely that associated topography has already subducted and interfered with the plate interface. However, independent evidence of subducted relief (Kodaira *et al*., 2002) only exists in isolated locations such as the subducted Papudo seamount along the extension of the Juan Fernandez Ridge (von Huene *et al*., 1997). Where we have found three or more topographic features with relief above a threshold value to align we have extrapolated their assumed linear trend into the subduction zone, taking into account offsets on known fracture zones. Moreover, we have assumed that in this case a topographic feature of a magnitude similar to that of the visible seafloor topography has already entered the subduction zone. The validity of this assumption can only be tested with targeted seismic surveys. The shallow dip of the seismogenic plate interface, ~18° on average (Tichelaar and Ruff, 1991), makes a correction for dip unnecessary near the plate boundary. Positive relief on the Nazca seafloor was contoured at 200 m intervals upward of 400 m, and contours were extrapolated into the subduction zone by projecting the widest parts of identified topography. Likely locations of subducted relief are shown in Figures 1 and 2.

Collocation of subducted topography and earthquake rupture endpoints

Rupturing in historical great earthquakes repeatedly arrested at 32°S and 15°S, on the subducted Juan Fernandez Ridge (JFR) and the Nazca Ridge respectively (Fig. 2). These ridges comprise the largest positive relief on the Nazca Plate. Other rupture limits are associated with subducted topography at 20°S, 25°S and 47°S. Specifically, 11 out of the

26 rupture limits in well documented great earthquakes were within 40 km of a zone with inferred subducted relief >1000 m, although only ~22% of the studied margin is within this distance. Whilst it has been possible for great earthquake ruptures to be located entirely between zones with high subducted relief (e.g., the 1939 event at 35° - 37°S), rupture zones generally do not appear to have crossed subducted relief >1000 m, with only one exception, the 1922 event which traversed an assumed obstruction at 28°S.

To test the statistical significance of our observations, we have compared the distribution of historical rupture zones with simulated patterns of rupture zones along the margin. Using a Monte Carlo approach, and observing that even in the absence of any subducted relief rupture limits from neighbouring earthquakes tend to collocate, forming subduction zone segments (Beck *et al.*, 1998), we have concatenated the rupture lengths of the thirteen sufficiently constrained historical earthquakes (not including the 2010 Maule earthquake), locating the first earthquake randomly along the South American margin, and repeating 2000 times. Two scenarios, representing end-member hypotheses for earthquake-topography interaction, were applied. In the first, 'unconstrained' scenario, subducted topography has no effect on rupture propagation. In this scenario, the next rupture in a sequence was started at the limit of the preceding earthquake.

This process was repeated to link 13 rupture zones, with rupture zone limits lying in nearby-pairs. The total length of this group exceeds the length of the margin along which the actual earthquakes occurred, due to overlap of ruptures over the record interval. Simulated rupture limits outside the geographic range of the historic earthquakes (12°S – 47°S) were discarded, and equal coverage along the margin was maintained. Note that proximity of rupture limits is a feature shared by most, but not all actual earthquake rupture zones (see Figure 2). Pairs of neighbouring rupture ends are a natural consequence of a segmented subduction zone in which earthquakes do not generally have overlapping rupture zones, irrespective of the mechanism of the segmentation.

In the second, 'constrained' scenario, rupture was stopped by subducted relief of a given minimum size H_{min}. The next earthquake rupture zone was located immediately beyond this relief. Relocated rupture limits were scattered at random within 50 km of the restricting topographic feature to represent the uncertainty of the actual observations. The alternative that earthquake rupture starts rather than stops on high subducted topography is not explored in detail for reasons given in the discussion, below.

If subduction of high standing seafloor topography has an effect on earthquake rupture propagation, then this effect may act some distance from the subducted feature, and the apparent width of a feature varies with H_{min}. To account for this, and for the uncertainty in the rupture endpoint location, we have varied the search distance S_D within which earthquake rupture endpoints are deemed to be associated with subducted topography. For a given search distance S_D and H_{min}, the simulation routine was repeated 2,000 times, generating a total of 26,000 earthquakes. The number of rupture limits for a specified S_D was normalized for comparison with the 26 limits of historic rupture zones. S_D was varied in steps of 5 km. H_{min} was varied in 200 m increments.

Historical data plot between the average results simulated for the constrained and unconstrained scenarios, and are close to the results of the constrained model at moderate relief, 800 – 1200 m, and search distances of 35 – 45 km (Fig. 3 a,b). This suggests that along the Nazca margin, features larger than 800 m commonly stop earthquake rupture propagation, and agrees with anecdotal observations.

An alternative test procedure, using earthquakes with $M_w \geq 8.0$ sampled randomly from the logarithmic Gutenberg-Richter relationship between earthquake magnitude and frequency rather than the historical earthquake catalogue, and assigning rupture area according to a common earthquake magnitude-length scaling law (Wells and Coppersmith, 1994), has yielded comparable results (supplementary information). A further alternative in which earthquakes were distributed individually rather than being linked together also produced equivalent findings.

Statistical significance of collocation

The collocation of historical rupture limits with subducted topography has not arisen by chance, according to a statistical significance test based on the probability density function of the distribution of simulated unconstrained earthquakes. In this test, we have determined the probability *P* that the number of rupture limits located within a given search distance S_D from subducted topography of a given size *H* for randomly positioned, unconstrained earthquakes exceeds the number of historical rupture limits that meet the same criteria.

Our underlying assumption is that the number of rupture limits falling randomly near topographic features (N_{uc}) can be determined directly from the unconstrained distribution of rupture zones. Within groups of 26 simulated earthquake limits (N_{total}), those within a given distance of subducted topography were counted, and their probability function $\mathbf{P}(N_{uc} \geq N_{real})$ was determined. The probability of the unconstrained simulation (N_{uc}) having at least as many rupture limits near significant topography as the actual data (N_{real}) is given by:

$$\mathbf{P}(reproduced) = \mathbf{P}(N_{uc} \geq N_{real}) = \sum_{n=N_{real}}^{n=N_{total}} \mathbf{P}(N_{uc} = n)$$

Figure 3c shows a diagonal region in S_D – H_{min} space in which correlation is strongest between relief and rupture endpoints. This is because increasing S_D and H_{min} concurrently causes the same area of the margin to be considered. The minimum relief at which subducted features affect the location of rupture limits is equivalent to the lowest relief within this domain of significant correlation. At this relief the number of subducted topographic features included is maximal, and S_D smallest, without adverse effect on the correlation.

For H >1000 m and S_D = 40 km, rupture limits and subducted topography are significantly correlated, with P = 1.4 % (Fig. 3c). Note that no features have a maximum positive relief between 800 m and 1200 m. This limits the precision with which we can define critical relief for rupture collocation. Relief >1000 m admits the same number of subducted features as >800 m, but the additional width of features caused by using the lower threshold does not increase the amount of collocation.

Subducted relief <800 m does not appear to stop or start earthquake rupture propagation. The Nazca plate has much topography with relief of 400 - 800 m, but at S_D = 40 km, P = 4.3 % *for H* >800 m, whereas P increases to 28 % *for H* >400 m, indicating the absence of significant correlation at this relief threshold. Nevertheless, subduction of topography <800 m may still affect the slip distribution in particular earthquakes (Kodaira *et al.*, 2002).

Discussion

Collocation of subducted topography and rupture limits could arise from rupture initiation or termination. Assuming that the epicenter location denotes the initiation of rupture, it can be determined whether topography starts or stops great earthquakes. Six out of thirteen studied earthquakes had epicenters within 40 km of topography with H>1000 m, whilst ~22 % of the margin lies within this distance (See Fig. 2). The chance of this occurring at random is 22 %, according to an analysis of the synthetic distribution of epicenters, equivalent to the analysis of endpoints summarized above. This correlation is much weaker than the match between rupture endpoints and topography. None of the six events have rupture zones which cross subducting topography, but in all rupture has extended away from the topography. Hence, the subduction of seafloor relief >800-1000 m is likely to impede or stop earthquake rupture, even if rupture nucleated on or near to that topography.

In the absence of significant subducting topography, earthquake rupture may be stopped by other factors, either structural (e.g. forearc structure or geometry of the slab) or because there is insufficient release of energy to propagate the rupture tip, even in the absence of any structural changes. In fact, for all of the 14 earthquakes considered here at least one of the endpoints was not close to subducted topography.

Effective and continued rupture arrest by subduction of high standing seafloor topography may require topographic features to be spaced at less than the width of the seismogenic zone. Along the Nazca margin, the width of this zone is ~100 km. Greater separation between topographic features of sufficient size within an alignment could leave gaps in the barrier to rupture propagation. This may be the case for the seamount chain at 28°S where features with relief >1000 m are up to 200 km apart. Its trend was crossed by the 1922 great earthquake, the only such traverse on record.

According to our findings it is likely that there is a causal link between subducted topography and great earthquake rupture limits. Along-margin rupture could be stopped by subducted topography either because it forms a strongly coupled patch within the seismogenic zone (Scholz and Small, 1997), too strong to break in the rupture, or because it forms a weak, aseismic patch (Bilek *et al*., 2003) which has no stored strain to release. Assuming that the long-term rate of shortening is uniform along the subduction margin, the local strength of the plate interface affected by subduction of topography may be reflected in the seismic moment release between great earthquakes, when these patches are expected to catch up with slip elsewhere along the margin. Strong patches are likely to have a relatively high rate of seismic moment release in small and intermediate size earthquakes in these intervals. Weak patches cannot accumulate elastic strain and are expected to have subdued background seismicity.

We have calculated the cumulative moment release between great earthquakes over 35 years since 1973, including all shallow, intermediate size earthquakes (depth<50 km, M_W 5.0-7.9) within a 0.5° moving window, but excluding aftershocks within two months of a great earthquake, as well as the largest intermediate event in each zone, which results in a more robust estimate (Frohlich, 2007) (Fig. 2). Five of six locations along the margin with subducted topography >1000 m have low background moment release. Instead, substantial background moment release tends to be concentrated at great earthquake rupture limits away from subducted topography, showing that segment boundaries do have residual strain and that subducting topography changes the way in which this is released. The anti-correlation of tall subducted topography and maxima of intermediate seismicity indicates that this topography usually acts to weaken the plate interface, promoting aseismic deformation and hence impeding earthquake rupture along the margin. Weak interplate coupling associated with subducted topography has been observed for the Nazca Ridge (Perfettini *et al*., 2010) and in Japan (Mochizuki *et al.*, 2008).

2010 Mw 8.8 Maule, Chile Earthquake

Along the Nazca margin there is one exception to the collocation of subducted, high seafloor topography and minimum background seismicity. At 32°S, potentially very tall (>2 km) subducted topography of the JFR coincides with a peak in background seismicity (Fig. 2). This location is of special interest because it is where northward rupture propagation in the 2010 Maule earthquake arrested. The hypocenter of this earthquake was located offshore at 35.8°S, 72.7°W, at an estimated depth of ~38 km, with a thrust mechanism, striking at 18°N, parallel to the margin and dipping 18° to the east (USGS NEIC Catalog). Aftershock locations indicate that the earthquake ruptured the Nazca margin over a length of ~600 km (Fig. 1), occupying a known seismic gap (Ruegg *et al*., 2002). Along the South American margin, its rupture length was exceeded in historical times only in the 1960 M_w 9.5 earthquake. Rupture extended northward to 33.1°S, overlapping the 1906 and 1985 rupture zones and stopping within 22 km of the subducted JFR. Although this is consistent with our finding that subducted topography >1,000 m is likely to stop rupture propagation, we believe that it is the presence of a strong patch in the plate interface, borne out by high intermediate seismicity at this location, rather than the weakening effect of subduction of seafloor topography that has arrested northward rupture propagation in 2010. Uniquely, this is also the location of a subducted fracture zone, a change in the gradient of the subducted slab (Barazangi and Isacks, 1976), and a transition from a sediment filled to starved trench with an associated change from subduction accretion to subduction erosion (Bangs and Cande, 1997). High background moment release at 32°S, and the elevated plate interface strength it implies are likely to be the compound effect of all these factors, indicating that the weakening effect of subduction of high seafloor topography can be drowned out by strengthening due to other asperities.

Rupture in the Maule earthquake propagated southward to 38.6°S, unimpeded by significant subducted topography. At its southern limit, the 2010 rupture area overlaps the northern edge of the 1960 rupture area, indicating that the earlier earthquake may not have released all stress in this area. The southern rupture limit coincides with a large peak in background seismicity, a pattern found in at least eight historic great earthquakes on the Nazca margin (Fig. 2).

Conclusions

Along the South American Nazca margin rupturing in great earthquakes is likely to be impeded by subducted topography with positive relief >1000 m, engaged in the seismogenic part of the plate interface. In general, this appears to be due to mechanical weakening of the plate interface, thus preventing the buildup of stresses required for the propagation of very large earthquakes. This effect may require the actual presence of a topographic feature within the seismogenic zone, and could dissipate after the feature has been transported through this zone. On the subducted Juan Fernandez Ridge it may be overprinted by other factors that have strengthened the plate interface sufficiently to arrest rupturing in the 2010 Maule earthquake. Along margin sections with subducted relief <800 m, rupturing in historical great earthquakes has been unimpeded. The length of such sections may impose an upper bound on the possible earthquake size, limiting hazard in some places. If this is true, then the largest earthquakes between the intersections of the Nazca and Juan Fernadez ridges and the South America plate margin will have rupture lengths no larger than 550 km (equivalent M_w9.1). In contrast, rupture could be unimpeded between the JFR and the Chile Rise, over a length of 1,450 km, enabling an earthquake rupture 33% longer than in the 1960 M_w9.5 event on this segment of the Nazca margin.

References Cited

Angermann, D., Klotz, J. and Reigber, C. Space-geodetic estimation of the Nazca–South America Euler vector, 1999. Earth Planet. Sci. Lett. 171, 329-334.

Bangs, N. L. and Cande S.C., 1997. Episodic development of a convergent margin inferred from structures and processes along the southern Chile margin, Tectonophys.16, 489-50

Barazangi, M. and Isacks, B. L., 1976. Spatial distribution of earthquakes and subduction of the Nazca plate beneath South America, Geology 4, 686-692.

Beck, S. L., Barrientos, S., Kausel, E. and Reyes, M. Source characteristics of historic earthquakes along the central Chile subduction zone, 1998. J. South Am. Earth Sci. 11, 115-129.

Bilek, S. L., Schwartz, S. Y. and DeSchon, H. R., 2003. Control of seafloor roughness on earthquake rupture behavior. Geology 31, 455-458.

Bilek, S. L., in press. Seismicity along the South-American subduction zone: Review of large earthquakes, tsunamis, and subduction zone complexity. Tectonophysics, doi: 10.1016/j.tecto.2008.02.037

Cisternas, M., Atwater, B.F., Torrejon, F., Sawai, Y., Machuca, G., Lagos, M., Eipert, A., Youlton, C., Salgado, I., Kamataki, T., Shishikura, M., Rajendran, C.P., Malik, J.K., Rizal, Y., and Husni, M., 2005. Predecessors of the giant 1960 Chile earthquake. Nature 437.

Cloos, M., Thrust-type subduction zone earthquakes and seamount asperities: A physical model for seismic rupture, 1992. Geology, 20, 601–604.

Comte, D., Eisenberg, A., Lorca, E., Pardo, M., Ponce, L., Saragoni, R., Singh, S.K., and Súarez, G., 1986. The 1985 central Chile earthquake: a repeat of previous great earthquakes in the region? Science, 233, 449-453.

Delouis, B., Monfret, T., Dorbath, L., Pardo, M., Rivera, L., Comte, D., Haessler, H., Caminade, J.P., Ponce, L., Kausel, E., and Cisternas, A., 1997. The M_w = 8.0 Antofagasta (northern Chile) earthquake of 30 July 1995: a precursor to the end of the large 1877 gap. Bull. Seismol. Soc. Am. 87, 427-445.

Frohlich, C., 2007. Practical suggestions for assessing rates of seismic-moment release. Bull. Seismol. Soc. Am. 97, 1158-1166.

Kelleher, J.A., 1972. Rupture zones of large South American earthquakes and some predictions. J. Geophys. Res. 77, 2087-2103.

Kelleher, J. A. and McCann, W., 1976. Buoyant zones, great earthquakes, and unstable boundaries of subduction. J. Geophys. Res. 81, 4885-4896.

Kodaira, S., Kurashimo, E., Park, J.-O., Takahashi, N., Nakanishi, A., S., M., Iwasaki, T., Hirata, N., Ito, K., and Kaneda, Y., 2002. Structural factors controlling the rupture process of a megathrust earthquake at the Nankai trough seismogenic zone. Geophys. J. Int. 149, 815-835.

Llenos, A. L. and McGuire, J. J., 2007. Influence of fore-arc structure on the extent of great subduction zone earthquakes. J. Geophys. Res. 112, B09301.

Loveless, J. P., Pritchard, M. E. and Kukowski, N., in press. Testing mechanisms of subduction zone segmentation and seismogenesis with slip distributions from recent Andean earthquakes. Tectonophysics doi:10.1016/j.tecto.2009.05.008

Marks, K. M. and Smith, W. H. F., 2007. Some remarks on resolving seamounts in satellite gravity. Geophys. Res. Lett. 34.

Mochizuki, K., Yamada, T., Shinohara, M., Yamanaka, Y. and Kanazawa, T., 2008. Weak interplate coupling by seamounts and repeating M~7 earthquakes. Science 321, 1184-1197.

Perfettini, H., Avouac, J-P., Tavera, H., Kositsky, A., Nocquet, J-M., Bondoux, F., Chileh, M., Sladen, A., Audin, L., Farber, D. L., and Soler, P., 2010. Seismic and aseismic slip on the Central Peru megathrust. Nature 465.

Ranero, C. R. and von Huene, R., 2000. Subduction erosion along the Middle America convergent margin. Nature 404, 748-752.

Ruegg, J. C., Campos, J., Madariaga, R., Kausel, E., de Chabelier, J.B., Armijo, R., Dimitrov, D., Georgiev, I., and Barrientos, S., 2002. Interseismic strain accumulation in south central Chile from GPS measurements, 1996-1999. Geophys. Res. Lett. 29, 12-1-4.

Scholz, C. H. and Small, C., 1997. The effect of seamount subduction on seismic coupling. Geology 25, 487-490.

Sladen, A., Tavera, H., Simons, M., Avouac, J.P., Konca, A.O., Perfettini, H., Audin, L., Fielding, E.J., Ortega, F., and Cavagnoud, R., 2009. Source model of the 2007 Mw 8.0 Pisco, Peru earthquake: Implications for seismogenic behavior of subduction megathrusts. J. Geophys. Res. 115, B02405.

Smith, W. H. F. and Sandwell, D. T., 1997. Global sea floor topography from satellite altimetry and ship depth soundings. Science 277.

Sobiesiak, M.M., 2000. Fault plane structure of the Antofagasta, Chile earthquake of 1995. Geophys. Res. Lett. 27, 581-584.

Song, T-R. A. and Simons, M., 2003. Trench-parallel gravity variations predict seismogenic behaviour in subduction zones. Science, 301, 630-633.

Spence, W., Mendoza, C., Engdahl, E. R., Choy, G.L. and Norabuena, E., 1999. Seismic subduction of the Nazca Ridge as shown by the 1996-97 Peru earthquakes. Pure Appl. Geophys. 154, 753-776.

Tavera, H., Buforn, E., Bernal, I., Antayhua, Y. and Vilacapoma, L., 2002. The Arequipa (Peru) earthquake of June 23, 2001. J. Seismol. 6, 279-283.

Tichelaar, B. W. and Ruff, L. J., 1991. Seismic coupling along the Chilean subduction margin. J. Geophys. Res. 96, 11997-12022.

USGS NEIC catalog: http://earthquake.usgs.gov/earthquakes/eqarchives/epic/
USGS Maule Earthqake: http://earthquake.usgs.gov/earthquakes/eqinthenews/2010/us2010tfan/

von Huene, R., and 47 coauthors, 1997. Tectonic control of the subducting Juan Fernandez Ridge on the Andean margin near Valparaiso, Chile. Tectonics 16, 474-488.

Wells, E. L. and Coppersmith, K.J., 1994. New empirical relationships among magnitude, rupture length, rupture width, rupture area, and surface displacement. Bull. Seismol. Soc. Am. 84, 974-1002.

Wells, R. E., Blakely, R. J., Sugiyama, Y., Scholl, D. W. and Dinterman, P. A., 2003. Basin-centered asperities in great subduction zone earthquakes: A link between slip, subsidence and subduction erosion? J. Geophys. Res. 10, 2507-2536.

Figure 1: Historic great subduction earthquakes along Pacific margin of South America. Where epicenters plot outside identified rupture zones, this is likely due to inaccuracies in locating earthquakes before the global installation of seismometers. Areas with more than 1000 m relief are marked on shaded seafloor topography. Black dots and lines show the inferred location of subducted topographic highs, grey regions show the area within 50 km of these highs. Inset: Detailed view of the area of the 27 February 2010 Maule earthquake. Red dots show aftershocks between February 27 and March 8, with size scaled by magnitude.

Figure 2: Latitudinal distribution of seismicity and subducted relief along Nazca margin. Earthquake rupture zones and epicenters are shown as black bars and white stars, respectively; thin black line is seismic moment release in $M_W<8.0$ earthquakes at depths less than 50 km since 1973 (0.5° moving windows). Also shown are areas with inferred subducted seafloor relief, binned at 200 m vertical intervals. Grey bars mark areas with likely subducted relief >1000 m, transposed to the upper axes for comparison. An exception to separation of relief and moment release is the JFR at 32°S.

Figure 3: Relation between (inferred) subducted seafloor relief and rupture limits in actual and simulated earthquake distributions. Circles show limits of 13 actual earthquake ruptures. Triangles and squares show results for simulations in which rupture limits are/are not constrained by subducted seafloor features, respectively. Synthetic results are based on 2000 runs with 13 earthquakes each. A) Number of earthquake limits within search distance from (inferred) subducted seafloor relief >1000 m. B) Number of earthquake ruptures within 40 km of (inferred) subducted seafloor relief of varying size. Error bars denote the inter-quartile range of the synthetic results. Note how the plot of observed earthquake rupture limits approaches that of topographically constrained, synthetic ruptures. C) Probability of the observed correlation of earthquake rupture limits and subducted seafloor relief being reproduced by chance by an unconstrained synthetic distribution. Strongest topography – rupture limit correlation (marked in white) occurs between 1000 - 1600m relief and 40 - 80km search distance. The diagonal nature of the domain with low *P* is due to a trade-off between relief and area searched; increasing relief narrows admitted topographic features, reducing the area searched for a given S_D.

Figure 1

Click here to download high resolution image

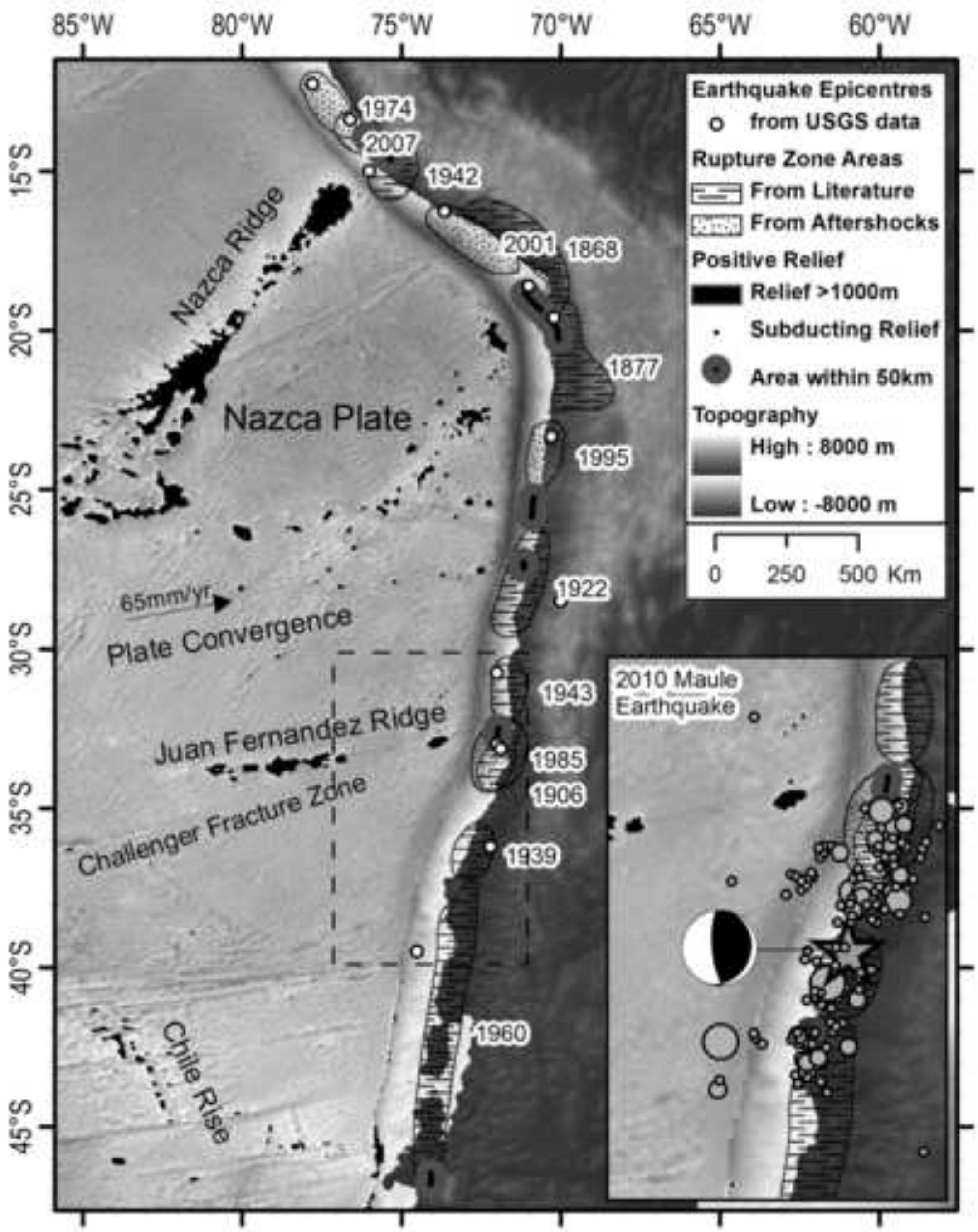

Figure 2
Click here to download high resolution image

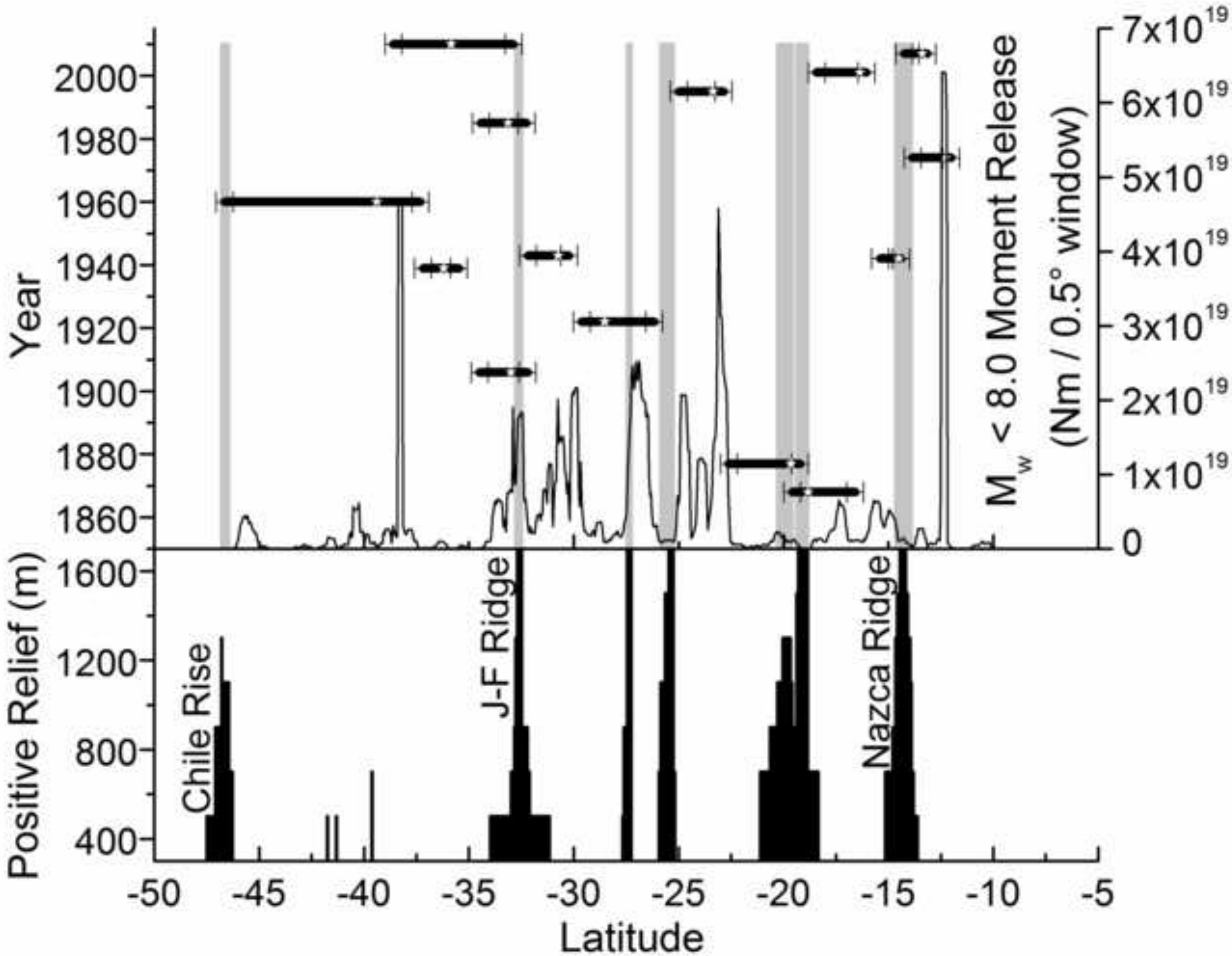

Figure 3
Click here to download high resolution image

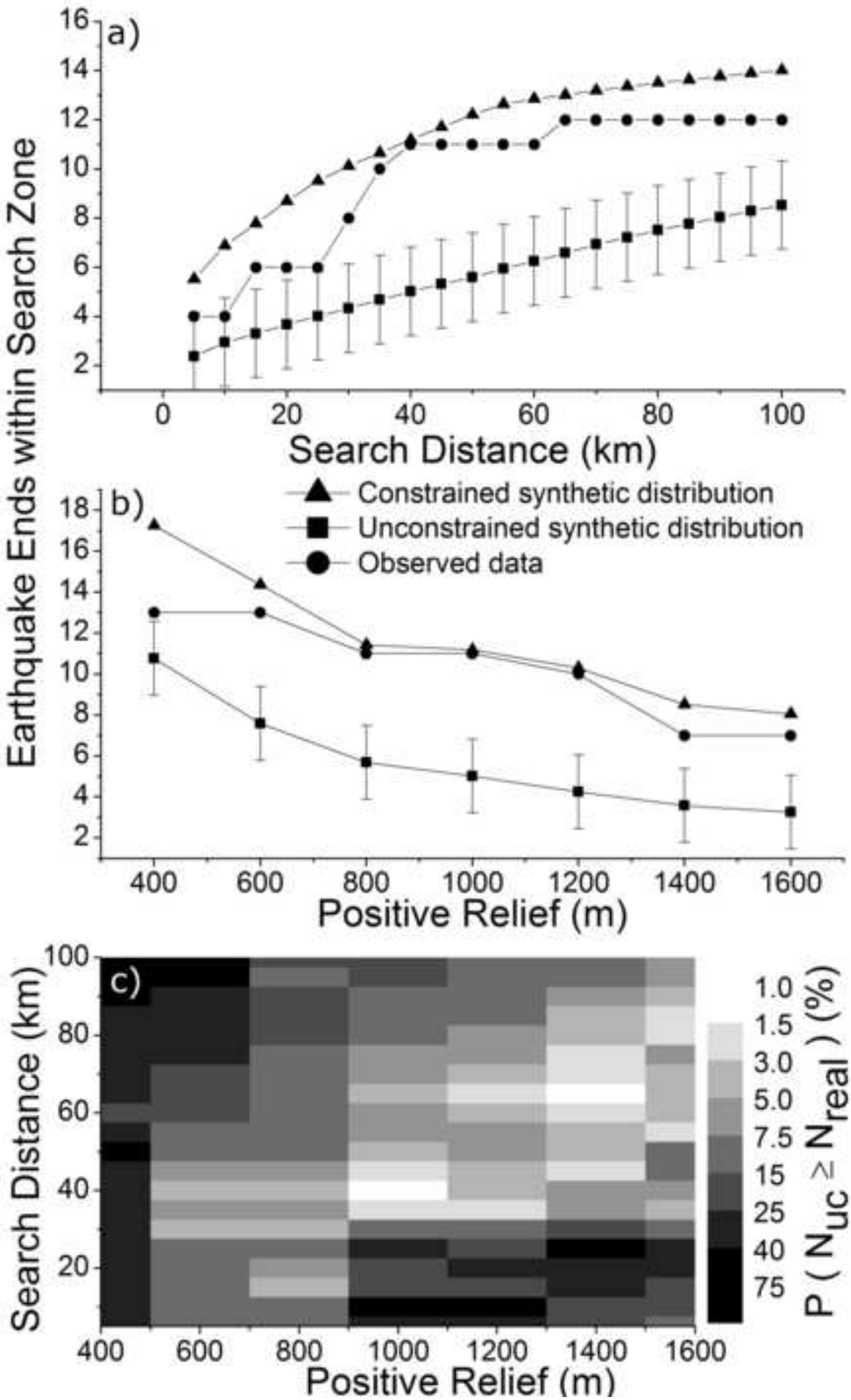

Table 1
Click here to download Table: Table1.xls

Date	Source	Alternate rupture zone estimation	Location	Magnitude	Length (km)
13/08/1868	Spence 1999		Southern Peru	8.8	400
10/05/1877	Spence 1999		Northern Chile	8.8	400
8/17/1906	Kelleher 1972		Central Chile	8.6	250
11/11/1922	Kelleher 1972		Central Chile	8.4	390
1/25/1939	Kelleher 1972		Southern Chile	8.2	190
8/24/1942	Kelleher 1972		Central Peru	8.6	150
4/6/1943	Kelleher 1972		Central Chile	8.3	210
5/22/1960	Cisternas 2005		Southern Chile	9.5	1050
10/3/1974	Aftershocks		Central Peru	8	280
3/3/1985	Aftershocks	Comte 1986	Central Chile	8	250
8/1/1995	Aftershocks	Delouis 1997, Sobesiak 2000	Northern Chile	8	240
6/23/2001	Aftershocks	Tavera 2001	Southern Peru	8.4	360
8/15/2007	Aftershocks		Central Peru	8	160

Supplementary Information:

Gutenberg-Richter distribution

As well as generating earthquake distributions using the rupture lengths from measured earthquakes, rupture lengths were assigned at random according to the logarithmic Gutenberg-Richter magnitude relationship. Earthquake magnitudes were converted into lengths using scaling factors based on the earthquake moment. Lengths varied from 100 km at magnitude 8.0 up to an artificially limited maximum rupture length of 1000 km at Mw 9.5 and above due to the lack of naturally-occurring earthquakes existing above this length.

After determining the rupture length, the synthetic earthquake rupture procedure continued as before, placing earthquakes in groups of 13 and rupturing these in sequence along the subduction margin. Earthquakes end points were allowed to rupture unrestricted, or to be restricted by projected subducting topographic features.

The results are similar to those obtained using the measured earthquake rupture zone lengths. At low relief, there is no correlation between rupture endpoints and topography, the observed number of rupture endpoints near to topography is reproducible by random positioning of synthetic endpoints. At moderate topographic heights (1000 – 1200 m) there is good correlation between rupture zone endpoints and a zone up to ~50km away from the topography.

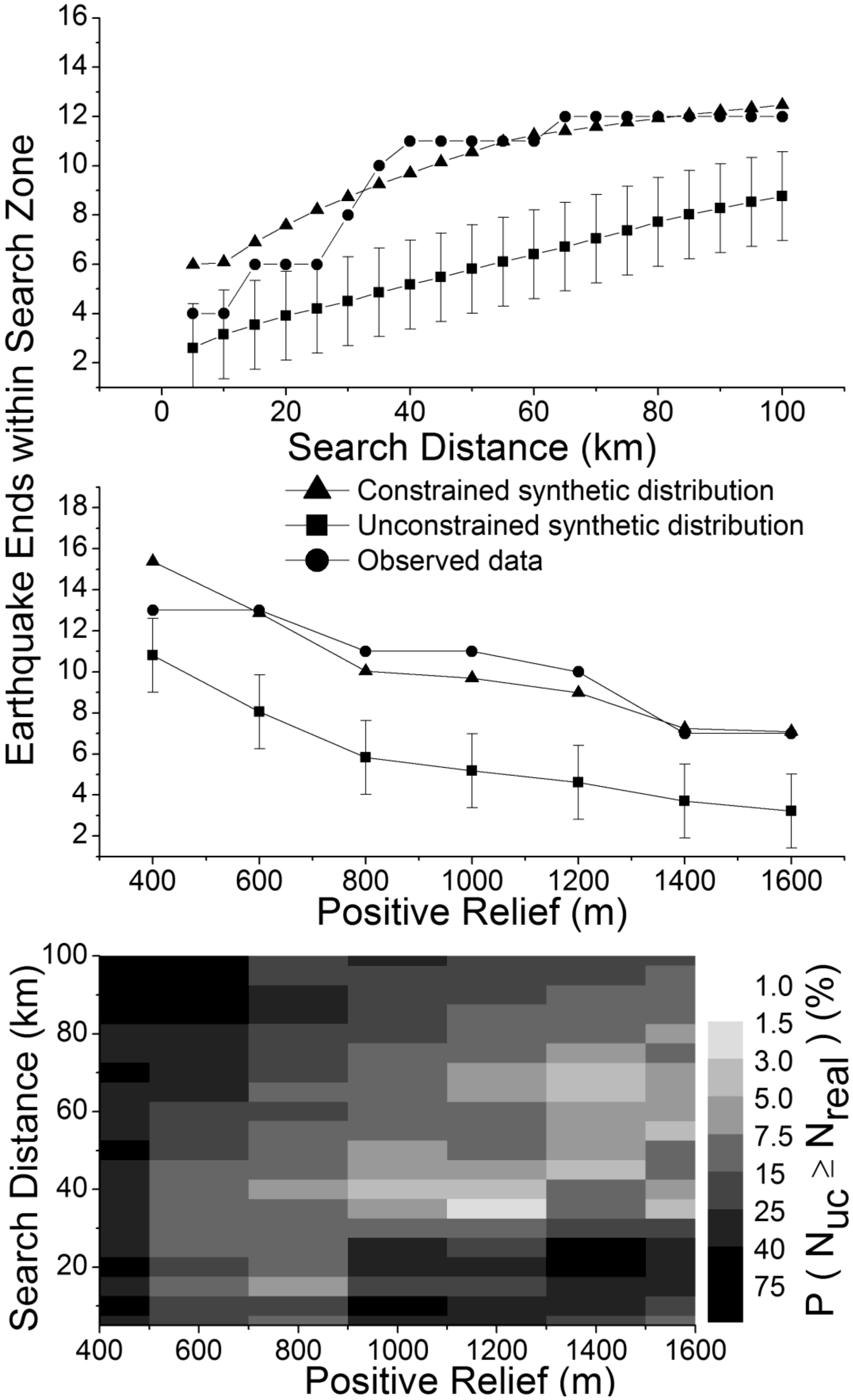

Earthquake Ends within Search Zone
Search Distance (km)
Constrained synthetic distribution
Unconstrained synthetic distribution
Observed data
Positive Relief (m)
Search Distance (km)
Positive Relief (m)
P ($N_{uc} \geq N_{real}$) (%)
1.0
1.5
3.0
5.0
7.5
15
25
40
75

Supplementary figure